Foraminiferal turnover across the Paleocene/Eocene boundary at the Zumaya section, Spain: record of a bathyal gradual mass extinction

Lamia Zili[1,*], Dalila Zaghbib-Turki[1], Laia Alegret[2], Ignacio Arenillas[2], and Eustoquio Molina[2]

[1] *Département de Géologie, Faculté des Sciences de Tunis, Université Tunis-El Manar, 2090, Tunisia.*
[2] *Departamento de Ciencias de la Tierra, Universidad de Zaragoza, 50009 Zaragoza, Spain.*
* lamia_2b@yahoo.fr

ABSTRACT

An integrated study of benthic and planktonic foraminiferal assemblages across the Paleocene/ Eocene boundary at the Zumaya section (Spain) has been carried out in order to analyse the short period that is commonly known as the Initial Eocene Thermal Maximum, and its impact on the foraminiferal assemblages. Benthic foraminiferal assemblages from uppermost Paleocene and lowermost Eocene sediments at the Zumaya section contain abundant representatives of the calcareous Velasco-type fauna and of the agglutinated flysch-type fauna, indicating a lower bathyal depth of deposition. The onset of the carbon isotope excursion, which marks the Paleocene/Eocene boundary, is recorded at the base of a 40-cm thick grey marly interval (unit U2), and it coincides with the beginning of a Benthic Foraminiferal Gradual Extinction. The pattern of extinction is adjusted more to a gradual and rapid episode rather than to a catastrophic sudden event as was proposed initially. The Paleocene/Eocene benthic foraminiferal extinction is followed by an acme of acarininids (among planktonic foraminifers) and of agglutinated benthic foraminifers, referred here as Agglutinated-Acarinina peak, which is interpreted as the result of global warming, carbonate corrosivity and environmental stress during the Initial Eocene Thermal Maximum. The occurrence of a dissolution interval above the extinction event, where agglutinated benthic foraminifers are abundant and calcareous foraminifers are scarce to absent, is compatible with the global rise of the lysocline and Calcite Compensation Depth in the lower Eocene, due to the increase in partial pressure of oceanic CO_2 and therefore, in the deep ocean water corrosiveness.

Key words: Acarinina, benthic foraminifers, gradual mass extinction, warming, late Paleocene, early Eocene, Zumaya section, Spain.

RESUMEN

Se realiza un estudio integrado de las asociaciones de foraminíferos bentónicos y planctónicos del límite Paleoceno/Eoceno en el corte de Zumaya (España) para analizar el corto periodo denominado máximo termal del Eoceno inicial, y su impacto en las asociaciones de foraminíferos. Las asociaciones de pequeños foraminíferos bentónicos de los sedimentos del Paleoceno terminal y del Eoceno inicial en Zumaya contienen abundantes representantes de la fauna calcárea de tipo Velasco y de la fauna aglutinada de tipo flysch, características de una profundidad de depósito batial inferior. El inicio del cambio isotópico, que marca el límite Paleoceno/Eoceno, está registrado en la base de un intervalo de margas grises (unidad U2) de 40 cm de potencia, y coincide con el comienzo de una Extinción Gradual de Foraminíferos Bentónicos. El patrón de extinción se ajusta más a un episodio gradual y rápido que a un evento súbito catastrófico como fue propuesto inicialmente. La extinción de los foraminíferos

bentónicos del Paleoceno/Eoceno es seguida por una abundancia de acarinínidos (entre los foraminíferos planctónicos) y de foraminíferos bentónicos aglutinados, referida en este trabajo como pico de Aglutinados-Acarinina, el cual es interpretado como el resultado del calentamiento global, corrosividad de carbonatos y desestabilización medioambiental durante el máximo térmico del Eoceno inicial. La presencia de un intervalo de disolución tras el evento de extinción, donde abundan los foraminíferos bentónicos aglutinados y los foraminíferos calcáreos son escasos o ausentes, es compatible con una subida global de la lisoclina y del nivel de compensación de la calcita en el Eoceno inferior debido al aumento de la presión parcial del CO_2 oceánico y, por tanto, de la corrosividad del las aguas profundas oceánicas.

Palabras clave: Acarinina, foraminíferos bentónicos, extinción masiva gradual, calentamiento, Paleoceno superior, Eoceno inferior, corte de Zumaya, España.

INTRODUCTION

During the last decades, much research has been focused on the Paleocene-Eocene interval transition, on the study of the rapidity and nature of the warming event that is associated to this interval, its ultimate cause, and its effects on the marine and terrestrial biota, including the mass extinction suffered by benthic foraminifers (see review by Thomas, 2007). This major extinction of benthic foraminifers is commonly known as the Benthic foraminiferal Extinction Event or BEE (Tjalsma, 1977; Schnitker, 1979; Tjalsma and Lohmann, 1983; Thomas, 1990), and its record has been traditionally placed at the Paleocene/Eocene (P/E) boundary. Benthic foraminiferal assemblages were indeed affected by a major environmental disturbance that has been related to the Initial Eocene Thermal Maximum (IETM, also known as the Paleocene Eocene Thermal Maximum, PETM) (*e.g.*, Thomas and Shackleton, 1996; Thomas *et al.*, 2000; Alegret *et al.*, 2005; Zachos *et al.*, 2005; Alegret and Ortiz, 2006). The benthic foraminiferal extinctions affected 30-50 % of the species in the deep sea (Thomas, 1990; Katz and Miller, 1991; Thomas and Shackleton, 1996; Thomas, 2007; Alegret *et al.*, 2009a, 2009b), whereas the extinctions were less severe in marginal and epicontinental basins (Thomas, 2003; Alegret *et al.*, 2005; Alegret and Ortiz, 2006). This benthic foraminiferal extinction occurred within a short period, with an estimated duration between ~3 and 17 kyr (Speijer *et al.*, 1997; Schmitz *et al.*, 1997; Kaiho *et al.*, 2006; Alegret *et al.*, 2009a, 2009b), shortly after a negative shift in $\delta^{13}C$ values (carbon isotope excursion, CIE) in bulk carbonate in marine and continental sections (Shackleton *et al.*, 1985; Kennett and Stott, 1991; Arenillas *et al.*, 1999; Röhl *et al.*, 2000; Thomas, 2003, 2007).

The most abrupt global warming event in the Cenozoic occurred in coincidence with the IETM, coeval with the BEE and the CIE (Zachos *et al.*, 2001, 2005). Several mechanisms have been proposed in order to explain the climate and geochemical anomalies across the IETM, the most plausible hypothesis being the dissociation of methane hydrates along the continental margins, which would increase the amount of $\delta^{13}C$-depleted carbon released into the atmospheric and oceanic reservoirs (Dickens *et al.*, 1995; 1997; Sluijs *et al.*, 2007; Thomas, 2007). In some sections, these anomalies are associated with dark organic-rich deposits (Speijer, 1994; Bolle *et al.*, 1999; Kaiho *et al.*, 2006; Aubry *et al.*, 2007), suggesting that the oxygen minimum zone occurred at the seafloor in some epicontinental basins across the P/E boundary. Oxygen depletion may have resulted from oxidation of methane in the ocean, local increased productivity or carbonate dissolution (Dickens *et al.*, 1997; Thomas, 2003, 2007; Kaiho *et al.*, 2006; Sluijs *et al.*, 2007; Zeebe and Zachos, 2007), triggering disturbance in benthic foraminiferal assemblages. A severe carbonate dissolution has been documented from many parts of the oceans in coincidence with the isotopic and geochemical anomalies (Canudo and Molina, 1992a, 1992b; Dickens *et al.*, 1997; Guernet and Molina, 1997; Arenillas and Molina, 2000; Alegret *et al.*, 2005; Thomas, 2007), and a 2 km rise of the Calcite Compensation Depth (CCD) has been inferred for the southeastern Atlantic (Zachos *et al.*, 2005; Thomas, 2007). Carbonate dissolution and shallowing of the CCD may also have resulted from methane oxidation in the ocean or atmosphere. However, there is no independent evidence for globally increased or decreased productivity or carbonate dissolution, nor for global anoxia or dysoxia (Thomas, 2007), and more studies are needed to understand the nature and consequences of the IETM. Isotopic and geochemical anomalies, carbonate dissolution and abrupt changes in foraminiferal assemblages linked to the IETM have been identified in Spanish sections (Molina *et al.*, 1994, 2003; Arenillas and Molina, 1996; Lu *et al.*, 1996; Alegret *et al.*, 2009a, 2009b), including the Zumaya section (Basque-Cantabrian Basin), which contains one of the most complete and expanded deep-water successions across the Paleocene-Eocene transition so far reported (Coccioni *et al.*, 1994; Canudo *et al.*, 1995; Ortiz, 1995; Orue-Etxebarria *et al.*, 1996; Sztràkos, 1996; Schmitz *et al.*, 1997; Pardo *et al.*, 1997; Molina *et al.*, 1999; Arenillas and Molina, 2000; Alegret *et al.*, 2009a). High resolution analyses of benthic foraminiferal assemblages carried out for the Zumaya section show that the P/E extinction affected 30 % to 55 % of abyssal and bathyal benthic foraminiferal species (Ortiz, 1995; Schmitz *et al.*, 1997; Alegret *et al.*, 2009a). This extinction, recorded in the middle part of the *Morozovella velascoensis* Biozone (Arenillas and Molina, 2000), also coincides with a negative shift in $\delta^{13}C$ (Schmitz

et al., 1997). In order to elucidate the benthic foraminiferal extinction pattern at the base of the IETM interval and to reconstruct the palaeoenvironmental evolution, we carried out a detailed study of benthic and planktonic foraminiferal assemblages across the Paleocene/Eocene boundary at the Zumaya section, and compared it with previous results on planktonic foraminifers.

Material and methods

The Zumaya section is located in northern Spain (43º18'00.35''N and 2º15'35.17''W), near the locality of Zumaya (Guipúzcoa province, Basque Country, western Pyrenees), on the Itzurun beach (Punta Mariantón). The access to the Zumaya section is easy by San Telmo beach (Figure 1). The Zumaya section contains one of the most complete and expanded deep-water successions across the Paleocene-Eocene transition (Molina *et al.*, 1999). For this reason, multidisciplinary studies have been carried out across the Paleocene-Eocene transition in this section, including magnetostratigraphic, isotopic, cyclostratigraphic and micropalaeontological analyses (Canudo *et al.*, 1995; Ortiz, 1995; Arenillas and Molina, 1996; Orue-Etxebarria *et al.*, 1996; Kuhnt and Kaminski, 1997; Schmitz *et al.*, 1997; Arenillas and Molina, 2000; Alegret *et al*., 2009a).

The total thickness of the studied section is 310 cm (Figure 2). We have distinguished five lithological units in this stratigraphical interval. The lower units (U1 and U2) were deposited during the latest Paleocene and the upper units (U3, U4 and U5) during the earliest Eocene:

- Unit U1 (50 cm) consists of decimetric-bedded grey marls-limestones and clay intercalations. It contains abundant well preserved planktonic and benthic foraminifers (Figure 2).

- Unit U2 (60 cm) consists of a massive grey calcareous bed, with a thin turbiditic bed at its base, below the benthic extinction event (Schmitz *et al.*, 1997, 2001).

- Unit U3 (40 cm) consists of grey marls. At the base of this unit (Z5), planktonic and benthic foraminifers are abundant and well preserved. Towards the top of unit U3 (Z6 and Z7), foraminiferal abundance and species richness decrease, and autochthonous foraminiferal calcareous tests are badly preserved and show partial dissolution.

- Unit U4 (150 cm) consists of reddish brown clays. This unit is rich in gypsum crystals (especially in samples Z8, Z9, Z13, Z15), and oxidized pyrite (*e.g.*, Z15 sample). At the base of this unit, the planktonic and benthic foraminifers are very rare (from Z9 to Z14). When they exist, the calcareous tests present differential dissolution features. Few specimens show pyritized tests (*e.g.*, *Tappanina selmensis* and *Nuttallides truempyi*).

- U5 (~20 cm) consists of reddish to grey clays rich in gypsum crystals. Foraminiferal tests are still affected by dissolution, but less intensely than in the previous interval.

Fourteen samples weighing 200 g were collected from the Zumaya section; these were spaced at 10 cm intervals close to the P/E boundary (*i.e.*, U3 and first half of U4) and
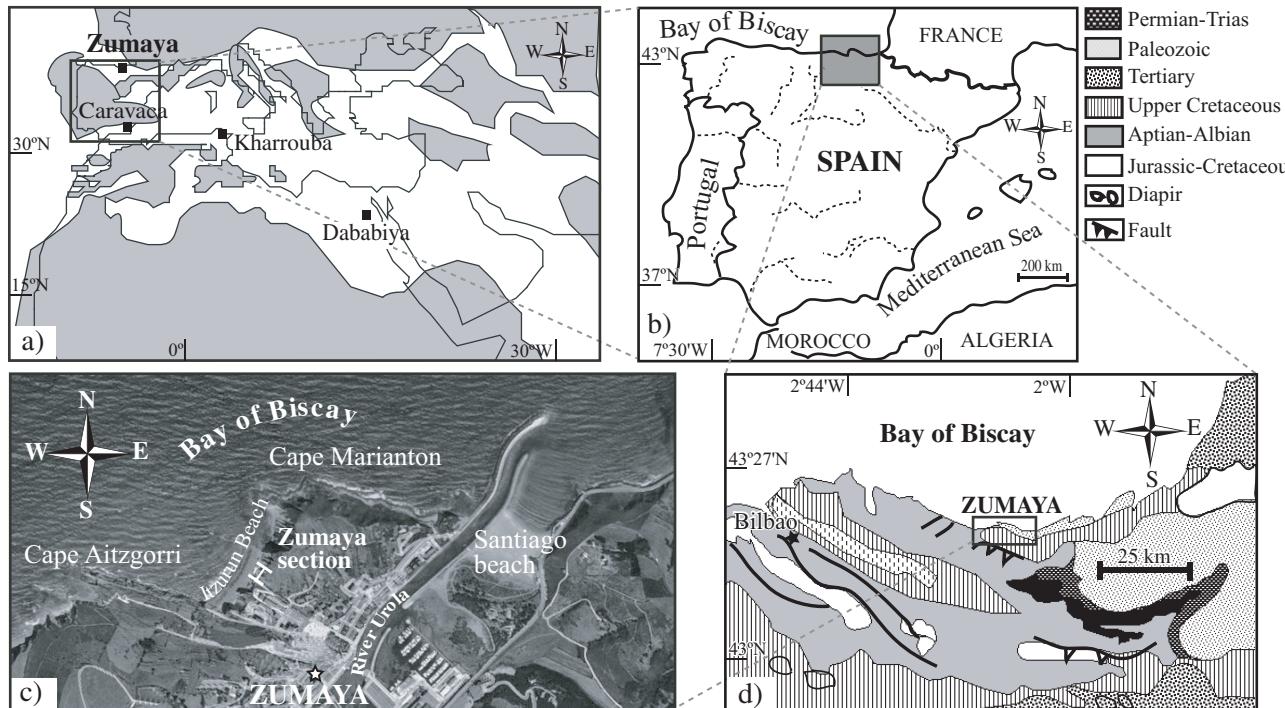
Figure 1. Palaeogeographical location of the Zumaya section during the IETM event (a). Geographic setting of the Zumaya section (b and c). Geological structures in the Zumaya area (d).
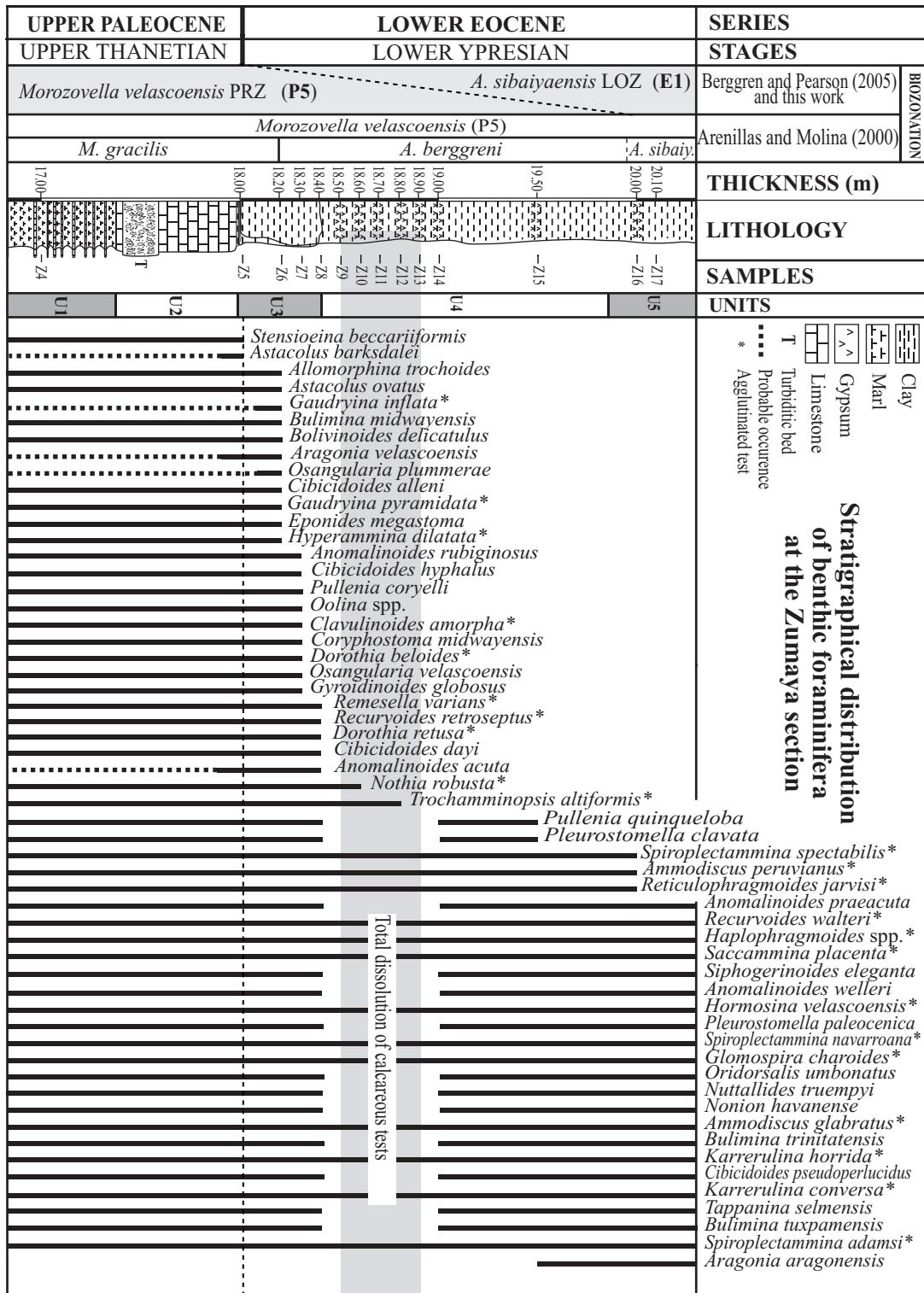
Figure 2. Benthic foraminiferal species range across the Paleocene-Eocene transition at the Zumaya section.

at 50 cm to 1 m intervals below and above it. All samples were washed through three sieves (250 µm, 100 µm and 63 µm) and the obtained residues were dried. When possible, about 300 specimens of benthic foraminifers were picked up (from Z4 to Z8 and from Z15 to Z17, see data on Table 1).

In sample Z4, the foraminifers were very abundant, for this reason an Otto micro-splitter was used allowing to obtain an available fraction occurring non-selective grained size and containing about 300 specimens. The total residues from the other samples (*i.e.*, from Z9 to Z14) were used because

the foraminifers there are very scarce and strongly affected by dissolution (<100 specimens per sample). Within the total dissolution interval, agglutinated tests dominate the assemblages because calcareous planktonic and benthic foraminiferal tests were completely dissolved. Calcareous-cemented, agglutinated foraminifera were also probably dissolved in this interval, which is therefore dominated by organic-cemented agglutinated foraminifera.

All counted species (Table 1) were mounted on micro-slides for a permanent record and deposited in the Invertebrate Paleontology, Paleoecology and Biostratigraphy Laboratory-Research Unit (DPS): 02/UR/10-02 at the

Faculty of Sciences of Tunis. Most of the identified species were photographed under a reflected light microscope. The planktonic foraminiferal quantitative information is based on data by Arenillas and Molina (2000). The environmental deposition at the Zumaya section may be deduced from the range and tolerance depth of species composing different benthic foraminiferal assemblages (Figure 2). Based on benthic foraminiferal data, we attempted to infer the palaeobathymetry, faunal turnover and pattern of extinction. The identification of benthic foraminiferal species is mainly based on Ellis and Messina (Catalogue of Micropalaeontology, 1940 to present), Tjalsma and

Table 1. Benthic foraminiferal specimens count from Zumaya section.

Samples	Z4	Z5	Z6	Z7	Z8	Z9	Z10	Z11	Z12	Z13	Z14	Z15	Z16	Z17
Thickness (m)	17.00	18.00	18.20	18.30	18.40	18.50	18.60	18.70	18.80	18.90	19.00	19.50	20.00	20.10
Allomorphina trochoides	0	1	2	0	0	0	0	0	0	0	0	0	0	0
Ammodiscus glabratus	19	4	5	0	4	0	0	0	0	0	0	1	0	1
Ammodiscus peruvianus	13	2	1	0	4	0	0	0	0	0	0	0	2	0
Ammobaculites jarvisi	0	0	0	0	0	0	0	0	0	3	0	0	0	0
Anomalinoides praeacuta	0	15	20	1	0	0	0	0	0	0	0	0	0	1
Anomalinoides acuta	0	8	0	7	1	0	0	0	0	0	0	0	0	0
Anomalinoides rubiginosus	3	0	1	2	0	0	0	0	0	0	0	0	0	0
Anomalinoides welleri	19	15	20	6	0	0	0	0	0	0	0	0	3	0
Anomalinoides spp.	0	13	18	24	1	0	0	0	0	0	0	1	0	0
Aragonia velascoensis	0	3	1	0	0	0	0	0	0	0	0	0	0	0
Aragonia aragonensis	0	0	0	0	0	0	0	0	0	0	0	3	7	14
Astacolus barksdalei	0	2	0	0	0	0	0	0	0	0	0	0	0	0
Astacolus ovatus	2	4	2	0	0	0	0	0	0	0	0	0	0	0
Bathysiphon spp.	10	10	8	17	20	3	0	0	2	0	0	7	11	24
Bolivina spp.	0	1	2	1	0	0	0	0	0	0	0	0	0	0
Bolivinoides delicatus	0	0	4	0	0	0	0	0	0	0	0	0	0	0
Bulimina midwayensis	0	0	1	0	0	0	0	0	0	0	0	0	0	0
Bulimina trinitatensis	0	0	1	0	0	0	0	0	0	0	0	0	0	0
Bulimina tuxpamensis	1	2	0	6	0	0	0	0	0	0	2	0	21	11
Bulimina spp.	0	3	2	1	0	0	0	0	0	0	0	2	2	0
Chrysalogonium spp.	4	0	5	0	0	0	0	0	0	0	0	3	0	0
Cibicidoides alleni	0	0	5	0	0	0	0	0	0	0	0	0	0	0
Cibicidoides dayi	1	0	3	0	1	0	0	0	0	0	0	0	0	0
Cibicidoides pseudoperlucidus	6	6	2	12	6	0	0	0	0	0	0	5	0	0
Cibicidoides hyphalus	0	4	10	2	0	0	0	0	0	0	0	0	0	0
Cibicidoides spp.	3	15	6	33	2	0	0	0	0	0	0	11	4	0
Clavulinoides amorpha	2	1	9	3	0	0	0	0	0	0	0	0	0	0
Coryphostoma midwayensis	6	7	3	8	0	0	0	0	0	0	0	0	0	0
Cyclammina pacifica	2	0	0	0	0	0	0	0	0	0	0	5	0	0
Dentalina spp.	17	30	22	27	0	0	0	0	0	0	0	3	0	0
Dorothia beloides	0	9	2	14	0	0	0	0	0	0	0	0	0	0
Dorothia retusa	0	8	3	2	1	0	0	0	0	0	0	0	0	0
Ellipsoidina spp.	0	0	3	0	1	0	0	0	0	0	0	0	0	0
Eponides megastoma	1	0	2	0	0	0	0	0	0	0	0	0	0	0
Fissurina spp.	1	1	3	4	0	0	0	0	0	0	0	0	0	0
Gaudryina pyramidata	0	0	3	0	0	0	0	0	0	0	0	0	0	0
Gaudryina inflata	0	0	2	0	0	0	0	0	0	0	0	0	0	0
Glomospira charoides	8	12	7	2	14	0	0	0	0	0	2	9	7	5
Globocassidulina spp.	0	0	0	14	5	0	0	0	0	0	2	7	32	23
Gyroidinoides globosus	8	0	3	10	0	0	0	0	0	0	0	0	0	0
Haplophragmoides spp.	15	6	2	26	108	0	4	0	0	0	3	4	4	3
Hormosina velascoensis	7	0	0	0	0	0	0	0	0	0	0	0	0	0
Hyperammina dilatata	5	0	3	0	0	0	0	0	0	0	0	0	0	0

Table 1 (Continued). Benthic foraminiferal specimens count from Zumaya section.

Samples Thickness (m)	Z4 17.00	Z5 18.00	Z6 18.20	Z7 18.30	Z8 18.40	Z9 18.50	Z10 18.60	Z11 18.70	Z12 18.80	Z13 18.90	Z14 19.00	Z15 19.50	Z16 20.00	Z17 20.10
Karrerulina conversa	8	1	5	2	5	0	0	2	2	0	0	2	2	1
Karrerulina horrida	7	4	7	7	20	1	0	4	0	0	1	11	22	0
Karrerulina spp.	0	8	0	0	0	0	0	0	0	0	0	7	10	4
Lenticulina spp.	9	3	6	11	1	0	0	0	0	0	0	0	0	0
Marginulina spp.	3	0	4	0	0	0	0	0	0	0	0	0	0	0
Nodosaria spp.	0	5	2	9	1	0	0	0	0	0	0	2	1	3
Nonionella spp.	0	0	2	1	0	0	0	0	0	0	0	0	0	0
Nonion havanense	2	1	3	0	0	0	0	0	0	0	0	0	0	0
Nonion durhami	1	0	0	0	0	0	0	0	0	0	0	0	0	0
Nothia robusta	16	0	0	0	9	0	16	0	0	0	0	0	0	0
Nuttallides truempyi	13	42	29	23	6	0	0	0	0	0	1	130	147	161
Oolina spp.	5	0	2	2	0	0	0	0	0	0	0	0	0	0
Oridorsalis umbonatus	6	3	3	5	1	0	0	0	0	0	0	0	0	0
Osangularia velascoensis	0	1	1	5	0	0	0	0	0	0	0	0	0	0
Osangularia plummerae	0	0	1	0	0	0	0	0	0	0	0	0	0	0
Pleurostomella spp.	6	2	4	3	0	0	0	0	0	0	0	3	0	0
Pleurostomella paleocenica	0	0	2	1	0	0	0	0	0	0	0	0	0	0
Pleurostomella clavata	0	0	0	1	0	0	0	0	0	0	0	2	0	0
Pullenia coryelli	2	7	1	2	0	0	0	0	0	0	0	0	0	0
Pullenia quinqueloba	0	0	0	6	0	0	0	0	0	0	0	2	0	0
Pyrulina spp.	5	2	0	0	0	0	0	0	0	0	0	0	0	0
Recurvoides walteri	0	0	0	0	0	2	0	0	0	0	0	16	18	18
Recurvoides retroseptus	2	21	14	0	7	0	0	0	0	0	0	0	0	0
Reticulophragmoides jarvisi	6	2	6	0	13	3	4	3	5	3	0	0	3	0
Reticulophragmoides spp.	0	0	0	0	17	0	4	0	0	0	0	0	0	0
Remesella varians	22	0	17	1	1	0	0	0	0	0	0	0	0	0
Saccammina placenta	9	3	0	1	11	2	6	2	0	0	1	5	8	6
Saccammina spp.	0	0	0	0	3	0	0	2	0	0	1	3	8	15
Siphogenerinoides eleganta	0	0	0	0	0	0	0	0	0	0	0	3	0	0
Spiroplectammina navarroana	9	9	1	0	3	0	0	4	1	0	0	6	2	0
Spiroplectammina spectabilis	9	4	4	0	0	0	0	0	0	0	0	1	1	0
Spiroplectammina adamsi	1	0	1	0	0	0	0	0	0	0	0	0	0	0
Spiroplectammina spp.	0	0	0	0	0	0	4	0	0	0	0	2	0	0
Stensioeina beccariiformis	4	1	0	0	0	0	0	0	0	0	0	0	0	0
Stilostomella spp.	2	0	0	0	0	0	0	0	0	0	0	0	0	0
Subreophax spp.	0	0	0	0	0	0	0	0	0	0	0	0	0	10
Tappanina selmensis	0	0	0	0	0	0	0	0	0	0	0	50	0	0
Trochamminopsis altiformis	0	2	0	0	4	1	4	5	1	0	0	0	0	0
Trochamminopsis spp.	0	0	0	0	0	0	4	0	0	2	0	0	0	0
Total specimens	**300**	**303**	**301**	**302**	**270**	**12**	**46**	**23**	**11**	**8**	**13**	**306**	**315**	**300**

Lohmann (1983), Van Morkhoven *et al.* (1986), Alegret and Thomas (2001), Kaminski and Gradstein (2005), Ortiz (2006), and Alegret and Ortiz (2006).

PLANKTONIC FORAMINIFERAL BIOSTRATIGRAPHY

Planktonic foraminiferal ranges and zonations

We have mainly used the planktonic foraminiferal zonations proposed by Molina *et al.* (1999) and Berggren and Pearson (2005). In Figure 3, we compare the recent P/E planktonic foraminiferal zonations for middle-low latitude areas. The most used standard P/E biozones (Figure 4), based on index species are *Luterbacheria pseudomenardii* (synonym of *Planorotalites*), *Morozovella velascoensis* and *Morozovella subbotinae* zones, named P4, P5 and P6 by Berggren *et al.* (1995). Berggren and Pearson (2005) proposed a new alphanumeric notation for the Paleogene zones, using the prefix "P" for the Paleocene zones and "E" for the Eocene ones (Figure 3). According to their zonal definitions, Biozone P5 spans *M. aequa*, *M. gracilis* and *A. berggreni* subzones by Molina *et al.* (1999), and E1 and E2 are equivalent to *A. sibaiyaensis* and *P. wilcoxensis* subzones by Molina *et al.* (1999), respectively. According to Berggren and Pearson (2005), the estimated ages of the lower and upper boundaries of E1 are 55.50 and 55.35 Ma, respectively. New astronomical calibrations of the Paleocene suggest an age of 55.53 to 56.33 Ma for the P/E boundary (Westerhold

Figure 3. Correlation between the proposed planktonic foraminiferal zonations for the Paleocene-Eocene transition, including the first occurrence data (FOD) and last occurrence data (LOD) of the used index species.

et al., 2008). A radiometric calibrated age of approximately 55.8 Ma for the P/E boundary was previously proposed by Westerhold *et al.* (2007), suggesting that the lower and upper boundaries of E1 are, respectively, 55.8 and 55.65 Ma, and the top of the revised section is approximately 55.74 Ma in age. According to Berggren and Pearson (2005), the lower boundary of E1 coincides with the P/E boundary (55.8 Ma), although this contradicts the biostratigraphical data from the Zumaya section.

The stratigraphical distribution of planktonic foraminiferal species across the P/E boundary at the Zumaya section is based on Arenillas and Molina (2000). The P/E boundary, officially defined in coincidence with the major negative excursion in $\delta^{13}C$, was recognized near the base of the carbonate dissolution interval and the main foraminiferal extinction horizon in the middle part of the chronozone C24r and the middle part of the *M. velascoensis* Zone (= P5 by Berggren *et al.*, 1995). The beginning of the $\delta^{13}C$ decrease precedes the main benthic foraminiferal disturbance horizon and the carbonate dissolution interval, and it approximately coincides with the base of the *A. berggreni* Subzone. The $\delta^{13}C$ negative shift is close to the base of the *A. sibaiyaensis* Subzone at the Zumaya section.

Quantitative stratigraphical distribution

The study of the quantitative stratigraphical distribution of species and genera by Arenillas and Molina (2000) showed relevant events across the P/E boundary at the Zumaya section. Their quantitative analyses indicated a major increase in low latitude acrininids coinciding with the CIE interval, similar to that recognized by Canudo and Molina (1992a) and Canudo *et al.* (1995). As illustrated in Figure 4, the *Acarinina* increase and the *Morozovella* decrease coincide with the $\delta^{13}C$ and $\delta^{18}O$ shifts across the P/E boundary at the Zumaya section (Figures 4 and 5), according to data by Schmitz *et al.* (1997) and Arenillas and Molina (2000).

The planktonic foraminiferal species richness is about 40 species per sample in the uppermost Paleocene, and assemblages suggest relatively temperate superficial waters, dominated by Atlantic currents. In the uppermost *Morozovella gracilis* Subzone, the relative abundance of *Morozovella* increases up to ~27 %, suggesting a slight increase of superficial water temperature. The lower part of the *A. berggreni* Subzone is characterized by rapid and gradual increase of *Acarinina*, reaching 39 % of the assemblages
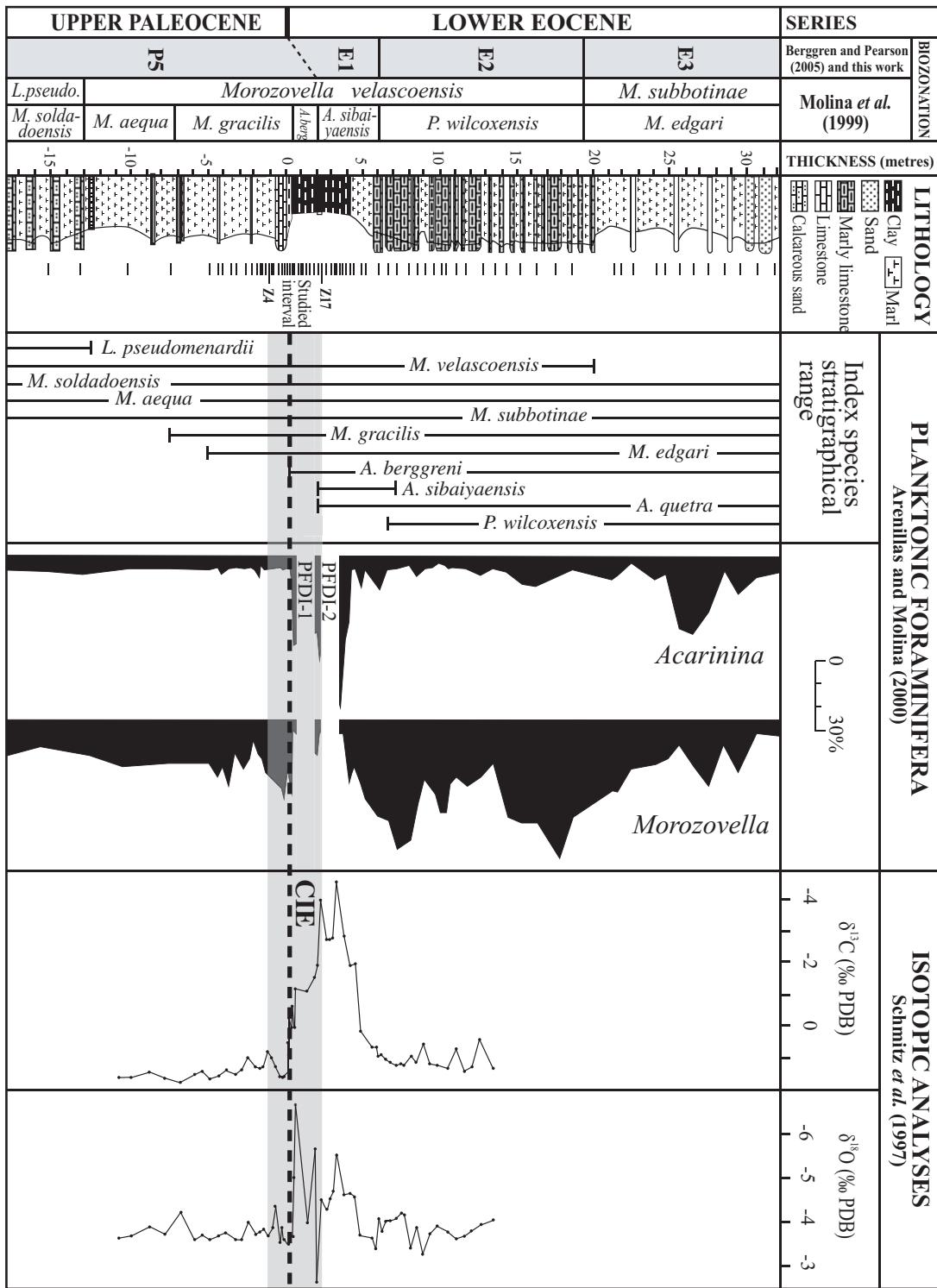
Figure 4. Stratigraphical ranges of planktonic foraminiferal index species, evolution of the relative abundances of *Acarinina* and *Morozovella*, and δ¹³C and δ¹⁸O isotopic stratigraphy across the Paleocene-Eocene transition at the Zumaya section. PFDI: planktonic foraminiferal dissolution interval. CIE: carbon isotopic excursion. Modified from Schmitz *et al.* (1997) and Arenillas and Molina (2000).

immediately below the planktonic foraminiferal dissolution intervals (Figure 5). This percentage is only surpassed by *Subbotina* (~50 %), whereas *Morozovella* decreases suddenly to ~4 % of the planktonic assemblages. The *Acarinina*

acme spans the *A. berggreni* and *A. sibaiyaensis* subzones (Arenillas and Molina, 2000; and Figure 4) and includes species such as *A. esnaensis*, *A. wilcoxensis*, *A. triplex*, *A. strabocella* and *A. apanthesma*. In this stratigraphical
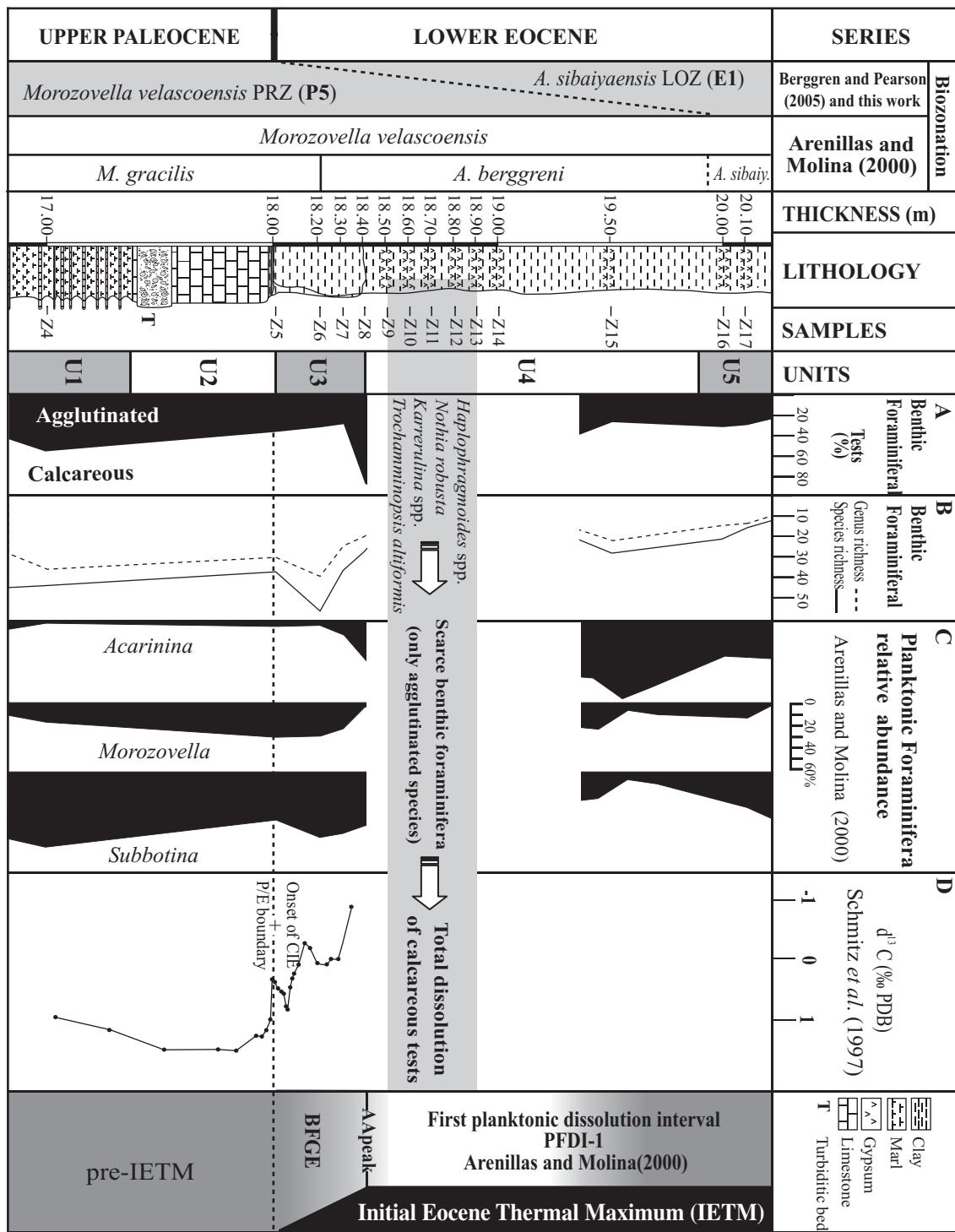
Figure 5. Percentage of benthic foraminifers with calcareous/agglutinated tests (A). Species and genus richness (B). Relative abundance of some planktonic foraminiferal taxa (C). Isotopic δ¹³C values across the Paleocene-Eocene transition at the Zumaya section (D). BFGE: Benthic foraminiferal Gradual mass Extinction. AApeak: Agglutinated-*Acarinina* peak.

interval, the first record of new compressed acarininids species occurs, including *A. berggreni*, *A. sibaiyaensis*, *A. africana* and *A. quetra*. Arenillas and Molina (2000) did not identify *Morozovella allisoniensis* at the Zumaya section. The evolution and proliferation of this species during the IETM (Kelly *et al.*, 1995, 1998; Speijer and Wagner, 2002)

seem to be restricted to tropical sea water.

Canudo and Molina (1992a), Canudo *et al.* (1995) and Arenillas and Molina (2000) noticed two planktonic foraminiferal dissolution intervals (PFDI-1 and PFDI-2) across the *A. berggreni* and *A. sibaiyaensis* subzones (Figure 4). Between these two dissolution intervals, they

identified a ~50 cm thick level in the lower part of the *A. sibaiyaensis* Subzone, corresponding to the unit U5 at the top of the revised section (Figure 5). This level contains planktonic foraminiferal assemblages with abundant *Acarinina* (~38 %) and *Subbotina* (~45 %), whereas percentages of *Morozovella* (~8 %) continue to be relatively low. The abundance of "large" morozovellids (including *M. velascoensis*, *M. acuta* and *M. parva*) seems to decrease across the *A. sibaiyaensis* and *P. wilcoxensis* subzones at the Zumaya section. The "large" morozovellids abundance decreases suddenly near the P/E boundary, from an average of ~5 % in the uppermost Paleocene to ~0.3 % across the IETM. Its abundance returns to ~2 % in the upper part of *M. velascoensis* Zone, but it does not reach the pre-P/E boundary values. On the contrary, the "small" morozovellid group (that includes *M. subbotinae*, *M. aequa*, *M. lacerti*, *M. gracilis*, *M. marginodentata* and *M. edgari*) increases in abundance before the IETM (Arenillas and Molina, 2000). At the Zumaya section, its pre-P/E abundance is ~14 % in average, its IETM abundance is ~6 %, and its post-IETM abundance is ~28 %. The biconvex morozovellids, *e.g.*, *M. occlusa* and *M.* cf. *albeari* (=*M. crosswicksensis* by Arenillas and Molina, 2000), show a quantitative distribution similar to the "large" morozovellids but with slightly lower values (pre-P/E abundance of ~2 %, IETM abundance of ~0.2 %, and post-IETM abundance of ~1.5 %).

PALAEOBATHYMETRY

Among calcareous taxa, representatives of the bathyal and abyssal Velasco-type fauna (Tjalsma, 1977; Tjalsma and Lohmann, 1983; Van Morkhoven *et al.*, 1986; Alegret *et al.*, 2003, 2009a) are common (*e.g.*, *Nuttallides truempyi*, *Aragonia velascoensis*, *A. aragonensis*, *Bulimina trinitatensis*, *B. tuxpamensis* and *Stensioeina beccariiformis*; Figure 2). The benthic assemblages also include abundant deep-water agglutinated taxa (Ortiz, 1995; Kaminski and Gradstein, 2005) such as *Karrerulina conversa*, *Spiroplectammina spectabilis*, *Haplophragmoides* spp., *Trochamminopsis* spp., *Glomospira charoides*, *Reticulophragmoides jarvisi* and *Hyperammina dilatata* (Figure 2). These agglutinated taxa represent more than 25 % of the assemblages (Figure 5A). On the basis of the benthic foraminiferal assemblages composition, we infer a lower bathyal environment of deposition for the uppermost Paleocene and lowermost Eocene at the Zumaya section, exceeding 600 m depth in agreement with Ortiz (1995) and Alegret *et al.* (2009a).

BENTHIC FORAMINIFERAL TURNOVER

The detailed analysis of benthic foraminifers from the Zumaya section allow us to identify several assemblages through the uppermost Paleocene and lowermost Eocene interval:

Uppermost Paleocene assemblages

Benthic foraminifers are abundant in the uppermost Paleocene, and their assemblages are very diversified (Figure 2). Units 1 and 2 contain mixed calcareous and agglutinated species. *Anomalinoides* (*A. welleri*, *A. rubiginosus*), *Cibicidoides pseudoperlucidus*, *Coryphostoma midwayensis*, *Nodosaria* spp., *Nuttallides truempyi*, *Dentalina* spp., *Lenticulina* spp., *Oridorsalis umbonatus* and *Stensioeina beccariiformis* are common among calcareous taxa. Diverse assemblages of agglutinated foraminifers such as *Ammodiscus glabratus*, *A. peruvianus*, *Bathysiphon* spp., *Nothia robusta* and *Spiroplectammina spectabilis* are also present. The benthic foraminiferal assemblages from the two basal units (U1 and U2) are dominated by infaunal morphogroups. These assemblages composition characterized by high species richness and various morphotypes indicate a normal-oxic environment and stable mesotrophic to oligotrophic conditions (Kaminski *et al.*, 1995; Jorissen *et al.*, 1995) at the seafloor during the deposition of Units U1 and U2 at the latest Paleocene.

Benthic foraminiferal gradual mass extinction (BFGE) in the earliest Eocene

The onset of the carbon isotope excursion, *i.e.*, the Paleocene/Eocene boundary, is recorded at the base of a grey clay interval at the Zumaya section (*i.e.*, at the base of U3; Figures 4 and 5d). A gradual pattern of Last Occurrence Data (LODs) of benthic foraminiferal species has been observed within the lower 40 cm of the clay interval (Z5-Z8 corresponding to unit U3, Figures 2 and 6):

(1) the LODs of *Stensioeina beccariiformis* and *Astacolus barksdalei* are recorded ~0–5 cm above the onset of the CIE;

(2) the LODs of species such as *Allomorphina trochoides*, *Astacolus ovatus*, *Gaudryina inflata*, *Bulimina midwayensis*, *Bolivinoides delicatulus*, *Aragonia velascoensis*, *Osangularia plummerae*, *Cibicidoides alleni*, *Gaudryina pyramidata*, *Eponides megastoma* and *Hyperammina dilatata* are observed ~20–25 cm above the onset of the CIE;

(3) the LODs of *Anomalinoides rubiginosus*, *Cibicidoides hyphalus*, *Pullenia coryelli*, *Clavulinoides amorpha*, *Coryphostoma midwayensis*, *Dorothia beloides*, *Osangularia velascoensis*, and *Gyroidinoides globosus* are recorded ~30–35 cm above the Paleocene/Eocene boundary;

(4) the LODs of *Remesella varians*, *Recurvoides retroseptus*, *Dorothia retusa*, *Cibicidoides dayi* and *Anomalinoides acuta* are observed ~40–45 cm above the onset of the CIE.

Some of these species (*e.g.*, *Gyroidinoides globosus*, *Stensioeina beccariiformis*, *Remesella varians*) have been documented to become extinct in the lowermost Eocene (Tjalsma and Lohmann, 1983; Van Morkhoven *et al.*, 1986),
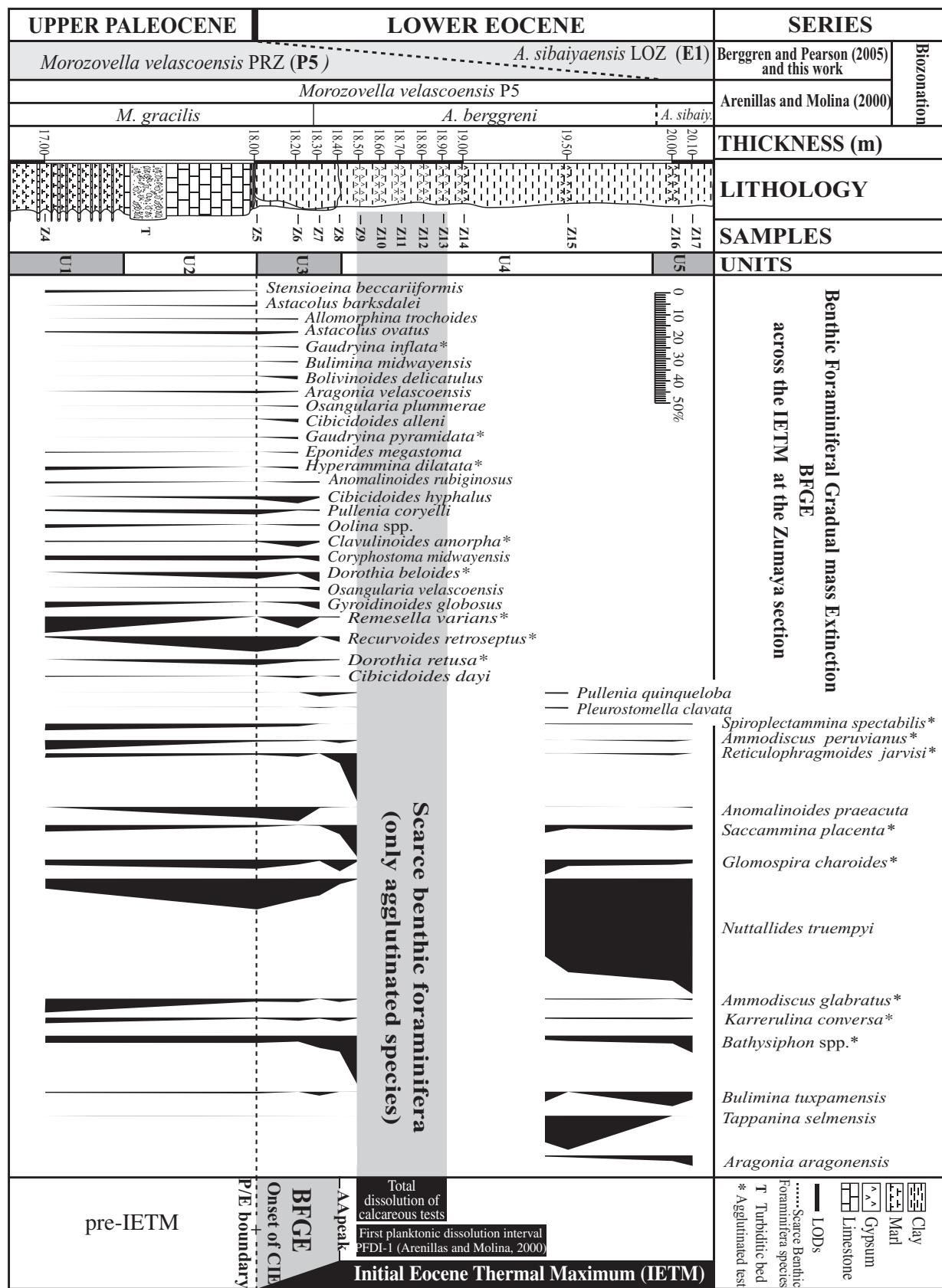
Figure 6. Distribution and quantitative data. Gradual extinction of benthic foraminiferal species across the Paleocene-Eocene transition at the Zumaya section. BFGE: Benthic foraminiferal Gradual mass Extinction, IETM: Initial Eocene Thermal Maximum. AApeak: Agglutinated-*Acarinina* peak.

and therefore their LODs represent not only local disappearances but also true extinctions. Previous studies on the Zumaya section suggest that the P/E benthic foraminiferal extinction affected 30 % to 55 % of deep-water benthic foraminiferal species (Ortiz, 1995; Schmitz *et al.*, 1997; Alegret *et al.*, 2009a). The LODs observed in this study reflect a gradual but rapid pattern of mass extinctions (Figures 2 and 6) which occurred within the grey clay interval (40 cm), with and estimated duration of ~17 kyr (Schmitz *et al.*, 1997).

In this grey clay interval (unit U3), the gradual pattern of extinction observed just after the negative excursion of $\delta^{13}C$ occurred when the environmental conditions were dramatically deteriorated (Speijer *et al.*, 1997; Alegret *et al.*, 2009a).

Benthic foraminiferal assemblages within the interval of total dissolution of calcareous tests

A ~50 cm-thick interval (at the base of unit U4; samples Z9 to Z13), where benthic foraminiferal tests are affected by intense carbonate dissolution, is recorded above the BFGE interval (~50 cm above the onset of the CIE). Within this dissolution interval, the different samples contain very few benthic foraminifers (8–46 specimens/ sample), and quantitative analysis from these samples is not reliable. For this reason, the percentages of the species and various benthic foraminiferal indices have not been plotted in Figure. 6. Only agglutinated benthic foraminifers such as *Karrerulina conversa*, *Bathysiphon* spp., *Ammobaculites jarvisi* and *Reticulophragmoides jarvisi* have been found within this interval. A similar dissolution interval has been identified in the neritic stratotype section for the P/E boundary in Dababiya Quarry (Egypt), where agglutinated benthic foraminifers may have taken advantage of a high-stress, probably strongly fluctuating environment (Alegret *et al.*, 2005; Alegret and Ortiz, 2006). Similarly, in addition to carbonate dissolution, environmental stress may have affected the benthos during deposition of the lower half of Unit 4 at the Zumaya section.

Benthic foraminiferal assemblages above the basal dissolution interval

Within the upper half of Unit 4 (Z14-Z15) several calcareous benthic foraminiferal specimens reappear, although their tests are still affected by dissolution suggesting that carbonate dissolution was not as intense as in the lower half of Unit 4.

In sample Z14, *Nuttallides truempyi* and *Bulimina tuxpamensis* show partial dissolution, whereas agglutinated taxa (*e.g.*, *Karrerulina horrida*, *Glomospira charoides*, *Saccammina placenta*) dominate the assemblages.

In sample Z15 benthic foraminifers are still affected

by dissolution. The relevant assemblage is oligotaxic, containing slightly more abundant and more diversified benthic foraminiferal species than Z14 assemblage. *Nuttallides truempyi* is relatively more abundant among those having calcareous hyaline tests (Figure 6). This epibenthic species may have been resistant to carbonate corrosivity (Jorissen *et al.*, 2007) and is also tolerant to oligotrophic conditions (Tjalsma and Lohmann, 1983; Nomura, 1991; Jorissen *et al.*, 1995; Speijer *et al.*, 1997; Alegret *et al.*, 2001; Thomas, 2007). Other calcareous (*e.g.*, *Anomalinoides praeacuta* and *Cibicidoides pseudoperlucidus*) and agglutinated epifaunal taxa (*e.g.*, *Glomospira charoides* and *Bathysiphon* spp.) are recorded within this interval suggesting more favourable conditions.

Abundant *Tappanina selmensis* and other taxa such as *Spiroplectammina* spp., *Bulimina tuxpamensis*, *Pleurostomella* spp., *Pullenia quinqueloba* and *Aragonia aragonensis* are also recorded in sample Z15 (Figure 6). *Tappanina selmensis* is common in the post-extinction interval, like at other sites and sections worldwide (*e.g.*, Thomas, 2007), and may indicate stressed seafloor conditions (Boltovskoy *et al.*, 1991; Takeda and Kaiho, 2007).

Assemblages from Unit 5 are strongly dominated by *Nuttallides truempyi*, pointing to oligotrophic conditions at the seafloor. Other common species are *Bulimina tuxpamensis*, *Aragonia aragonensis* and *Tappanina selmensis* among calcareous taxa, and *Reticulophragmoides jarvisi*, *Spiroplectammina*, *G. charoides*, *Bathysiphon*, *Ammodiscus*, and *Saccammina placenta* among agglutinated taxa.

DISCUSSION

The benthic foraminiferal assemblages from upper Paleocene and lower Eocene sediments at the Zumaya section contain abundant representatives of the Velasco-type fauna and the agglutinated flysch-type fauna, and indicate a lower bathyal depth of deposition, in agreement with Ortiz (1995). The benthic and planktonic foraminiferal assemblages show major disturbance and turnover across the Paleocene-Eocene transition at the Zumaya section. The upper Paleocene (upper part of the *M. gracilis* Subzone) is characterized by diversified assemblages of planktonic foraminifers, which are dominated by subbotinids and "large" morozovellids. These planktonic foraminiferal assemblages indicate relatively temperate surface waters, dominated by Atlantic currents. The benthic foraminiferal assemblages are diverse, and they contain mixed calcareous and agglutinated species of the Velasco-type fauna. These assemblages suggest normal conditions and environmental stability in surface waters as well as at the seafloor. The benthic foraminiferal assemblages during the upper Paleocene are highly diversified and indicate oxygenated and mesotrophic to oligotrophic conditions at the seafloor. Moreover, the occurrence of abundant species with calcareous tests indicates deposition above the CCD.

The IETM is marked, at the Zumaya section, by a red clayey bed in which the CIE is recorded (Schmitz *et al.*, 1997). A several per mille negative excursion in marine and terrestrial $\delta^{13}C$ values (which is recorded at sites and sections worldwide, as in Zumaya), is related to a rapid input of isotopically light carbon into the ocean-atmosphere system. Several hypotheses have been proposed to account for this input, being the massive dissociation of marine methane hydrates (Dickens *et al.*, 1995) the most widely accepted one. Dissociation of marine methane hydrates has been related to changes in ocean circulation, continental slope failure in the North Atlantic Ocean, sea-level drop, impact of an extraterrestrial body, volcanism, or to a combination of these factors (see references in Thomas, 2007; Moore and Kurtz, 2008). The ultimate causes of the CIE and of the global warming recorded across the IETM are beyond the scope of this paper. However, analysis of benthic and planktonic foraminiferal turnover may throw light on the environmental consequences of the IETM.

It is broadly accepted that the foraminiferal turnover at the Zumaya section, especially the quantitative acme of the planktonic foraminifers *Acarinina* spp. and the severe benthic foraminiferal extinction, was likely caused by the palaeoenvironmental changes related to the IETM (Canudo *et al.*, 1995; Schmitz *et al.*, 2001; Alegret *et al.*, 2009b). According to these data, the IETM begins at the base of the *A. berggreni* Subzone. The *Acarinina* species proliferating across the IETM (*A. esnaensis*, *A. wilcoxensis*, *A. triplex*, *A. strabocella* and *A. apanthesma*) are common in warm waters of the Tethys, suggesting that the *Acarinina* excursion in the Tethyan region was also related to increased global temperatures (Molina *et al.*, 1999). However, other tropical-subtropical groups such as "large" and biconvex morozovellids suddenly decreased in abundance (Arenillas and Molina, 2000), suggesting that the palaeoenvironmental changes during the IETM were probably more complex and other environmental factors (nutrients, water corrosivity, oxygenation, symbionts, *etc*.) affected the planktonic foraminiferal assemblages.

The gradual –but rapid– pattern of extinction of benthic foraminifers at the Zumaya section suggests that rapid (~10 kyr to ~17 kyr; Schmitz *et al.*, 1997; Alegret *et al.*, 2009a) palaeoenvironmental changes occurred at the beginning of the IETM. The onset of the mass extinctions coincides with the onset of the CIE and is close to the planktonic foraminiferal turnover, suggesting that all these events are linked. Consequently, the *A. berggreni* Subzone is a very significant stratigraphical interval. The BFGE is followed by a sudden increase in the relative abundance of agglutinated taxa and acarininids. We have designated the Agglutinated-*Acarinina* peak as the AApeak, representing the horizon where the increase in agglutinated benthic foraminifers and planktonic acarininids are first recorded (Figures 5A and 5C), although these acmes continue upward across the red clayey bed (Arenillas and Molina, 2000). This horizon seems to mark a first thermal maximum pulse

across the basal part of the IETM interval, although global warming and other palaeoenvironmental changes started before (Zachos *et al.*, 2003; Giusberti *et al.*, 2007; Sluijs *et al.*, 2007).

Succeeding this gradual extinctions (BFGE) interval, the base of the red clayey bed coincides with the base of a dissolution interval. This later interval contains oligotaxic benthic foraminifera assemblage composed of only agglutinated specimens. This assemblage is typical of environments with undersaturated carbonate waters, which are deposited below the CCD. Moreover, these oligotaxic assemblages may indicate stressed conditions at the sea floor.

The carbonate dissolution intervals might be the result of a progressive global rise of the lysocline and CCD, due to the increased partial pressure of CO_2, and therefore, of the deep ocean water corrosiveness (Dickens *et al.*, 1997; Arenillas *et al.*, 1999; Arenillas and Molina, 2000; Dickens, 2001).

The CCD may have reached the bottom waters shortly after the beginning of the IETM at Zumaya, initiating the total dissolution interval that is recorded at the base of the red clayey bed (see Arenillas and Molina, 2000). However, calcareous benthic foraminiferal tests are well preserved below the dissolution interval, and the gradual and rapid pattern of extinctions of benthic foraminifers reported here, which started well below the dissolution interval, suggests that carbonate corrosiveness was not the main cause of the benthic foraminiferal extinctions event. The beginning of the BFGE is recorded at the onset of the CIE, indicating that some kind of environmental stress, not related to carbonate dissolution, triggered the benthic foraminiferal extinctions. Severe global warming is the only major cause that may have induced the benthic foraminiferal disturbance in all oceans and at all latitudes (Thomas, 2007; Alegret *et al.*, 2009a, 2009b).

Although there are some samples where calcareous foraminiferal tests can be found (*e.g.*, samples Z15, Z16, Z17), the dissolution interval spans all red clayey beds in the uppermost *A. berggreni* and *A. sibaiyaensis* subzones. Across this interval, the assemblages are still dominated by agglutinated taxa, but some small-sized calcareous benthic foraminifers have been identified (*e.g.*, *Tappanina selmensis*, *Nuttallides truempyi* and *Aragonia aragonensis*). This size reduction affecting the benthic foraminiferal tests was probably related to environmental stress.

The acme of agglutinated taxa and acarininids continues at the Zumaya section above the dissolution interval, in the upper part of the *A. sibaiyaensis* Subzone (Canudo *et al.*, 1995; Arenillas and Molina, 2000). The relative abundance of morozovellids increases (Figure 4), but "large" and biconvex morozovellids (*e.g.*, *M. velascoensis*, *M. acuta*, *M. occlusa*) are progressively replaced by the "small" morozovellids group (*e.g.*, *M. aequa*, *M. subbotinae*, *M. edgari*) across the *P. wilcoxensis* Subzone (see Arenillas and Molina, 2000).

Benthic foraminiferal species richness is still low

towards the top of the studied interval (Figure 5B), suggesting that environmental conditions at the seafloor had not recovered in the *A. sibaiyaensis* Subzone. The benthic foraminiferal turnover at the Zumaya section is compatible with a rapid onset of the IETM anomalies lasting a time period <20 kyr as documented by Röhl *et al.* (2000). However, a return to more normal conditions occurred over longer time scales.

CONCLUSIONS

The benthic and planktonic foraminiferal turnover across the Paleocene-Eocene transition at the Zumaya section illustrates the impact of the IETM on lower bathyal foraminiferal dwellers. A gradual –but rapid– pattern of benthic foraminiferal mass extinctions (BFGE) has been identified. The base of this gradual extinctions interval coincides with the onset of CIE (*i.e.*, with the P/E boundary). The top of this interval coincides with the base of a dissolution one. A global cause, such as warming of the oceans, must have triggered the benthic foraminiferal mass extinctions in all oceans and all latitudes.

We identified the Agglutinated-*Acarinina* peak (AApeak) 40 cm above the P/E boundary. This represents the horizon where the increase in agglutinated benthic foraminifers and planktonic acarininids are first recorded, although these acmes continue upward across the red clayey bed. The *Acarinina* species thriving across the IETM suggest a rise of tropical-subtropical taxa toward higher latitudes; thus we speculate that the AApeak might mark a first thermal maximum pulse in the basal part of the IETM interval, although global environmental changes (such as global warming) started earlier, possibly triggering the benthic foraminiferal mass extinctions.

A dissolution interval, containing oligotaxic agglutinated benthic foraminiferal assemblages, spans the *A. berggreni* Subzone and the *A. sibaiyaensis* Subzone. Carbonate dissolution might be the result of a progressive upward migration of the lysocline and CCD due to the increased partial pressure of CO_2, possibly resulting from methane oxidation in the ocean or atmosphere.

The species richness of the benthic foraminiferal assemblages is still low towards the top of the studied interval (~55.44 Ma), suggesting that environmental conditions at the seafloor had not yet entirely recovered.

ACKNOWLEDGEMENTS

REFERENCES

Alegret, L., Ortiz, S., 2006, Global extinction event in benthic foraminifers across the Paleocene/Eocene boundary at the Dababiya Stratotype section: Micropaleontology, 52, 433-447.

Alegret, L., Thomas, E., 2001, Upper Cretaceous and lower Paleogene benthic foraminifers from northeastern Mexico: Micropaleontology, 47, 269-316.

Alegret, L., Molina, E., Thomas, E., 2001, Benthic foraminifers at the Cretaceous/Tertiary boundary around the Gulf of Mexico: Geology, 29, 891-894.

Alegret, L., Molina, E., Thomas, E., 2003, Benthic foraminiferal turnover across the Cretaceous/Paleogene boundary at Agost (southeastern Spain): paleoenvironmental inferences: Marine Micropaleontology, 48, 251-279.

Alegret, L., Ortiz, S., Arenillas, I., Molina, E., 2005, Paleoenvironmental turnover across the Paleocene/Eocene boundary at the Stratotype section in Dababiya (Egypt) based on benthic foraminifers: Terra Nova, 17, 526-536.

Alegret, L., Ortiz S., Orue-Etxebarria X., Bernaola G., Baceta J.I., Monechi S., Apellaniz E., Pujalte V., 2009a, The Paleocene-Eocene Thermal Maximum: new data from the microfossil turnover at the Zumaia section, Spain: Palaios, 24, 318-328.

Alegret, L., Ortiz, S., Molina, E. 2009b, Extinction and recovery of benthic foraminifera across the Paleocene-Eocene Thermal Maximum at the Alamedilla section (Southern Spain): Palaeogeography, Palaeoclimatology, Palaeoecology, 279, 186-200.

Arenillas, I., Molina, E., 1996, Bioestratigrafía y evolución de las asociaciones de foraminíferos planctónicos del tránsito Paleoceno-Eoceno en Alamedilla (Cordilleras Béticas): Revista Española de Micropaleontología, 18, 85-98.

Arenillas, I., Molina, E., 2000, Reconstrucción paleoambiental con foraminíferos planctónicos y cronoestratigrafía del tránsito Paleoceno-Eoceno de Zumaya (Guipúzcoa): Revista Española de Micropaleontología, 32, 283-300.

Arenillas, I., Molina, E., Schmitz, B., 1999, Planktic foraminiferal and $\delta^{13}C$ isotopic changes across the Paleocene/Eocene boundary at Possagno (Italy): International Journal of Earth Sciences, 88, 352-364.

Aubry, M.P., Ouda, K., Dupuis, C., Berggren, W.A., Van Couvering, J.A., Ali, J., Brinkhuis, H., Gingerich, P.R., Heilmann-Clausen, C., Hooker, J., Kent, D.V., King, C., Knox, R.W.O.B., Laga, P., Molina, E., Schmitz, B., Steurbaut, E., Ward, D.R., 2007, The Global Standard Stratotype-section and Point (GSSP) for the base of the Eocene Series in the Dababiya section (Egypt): Episodes, 30, 271-286.

Berggren, W.A., Pearson, P.N., 2005, A revised tropical to subtropical Paleogene planktonic foraminiferal zonation: Journal of Foraminiferal Research, 35, 279-298.

Berggren, W.A., Kent, D.V., Swisher, C.C., Aubry, M.P., 1995, A revised Cenozoic geochronology and chronostratigraphy, *in* Berggren, W.A., Kent, D.V., Hardenbol, J. (eds.), Geochronology, Time Scales and Global Stratigraphic Correlations: A Unified Temporal Framework for an Historical Geology: Society of Economic Paleontologists and Mineralogists, Special Volume 54, 129-212.

Bolle, M.P, Addate, T., Keller, G., Von Salis, K., Burns, S., 1999, The Paleocene-Eocene transition in the southern Tethys (Tunisia) climatic and environmental fluctuations: Bulletin de la Société géologique de France, 170, 661-680.

Boltovskoy, E., Scott, D.B., Medioli, F.S., 1991, Morphological variations of benthic foraminiferal tests in response to changes in ecological parameters, a review: Journal of Paleontology, 65, 175-185.

Canudo, J.I., Molina, E., 1992a, Planktic foraminiferal faunal turnover and bio-chronostratigraphy of the Paleocene-Eocene boundary at Zumaya (Northern Spain): Revista de la Sociedad Geológica de España, 5, 145-157.

Canudo, J.I., Molina, E., 1992b, Biostratigrafía con foraminíferos planctónicos del Paleógeno del Pirineo: Neues Jahrbuch für Geologie und Paläontologie, Abhandlungen, 186, 97-135.

Canudo, J.I., Keller, G., Molina, E., Ortiz, N., 1995, Planktic foraminiferal turnover and $\delta^{13}C$ isotopes across the Paleocene-Eocene transition at Caravaca and Zumaya, Spain: Palaeogeography, Palaeoclimatology, Palaeoecology, 114, 75-100.

Coccioni, R.D, Leo, R., Galeotti, S., Monechi, S., 1994, Integrated biostratigraphy and benthic foraminiferal faunal turnover across the Paleocene-Eocene boundary at Trabakuea Pass section, Northen Spain: Paleopelagos, 4, 87-100.

Dickens, G.R., 2001, Carbon addition and removal during the Late Paleocene Thermal Maximum: basic theory with a preliminary treatment of the isotope record at ODP Site 1051, Blake Nose, *in* Kroon, D., Norris, R.D., Klaus, A. (eds.), Western North Atlantic Paleogene and Cretaceous Palaeoceanography: The Geological Society of London, Special Publications 183, 293-305.

Dickens, G.R., O'Neil, J.R., Rea, D.K., Owen, R.M., 1995, Dissociation of oceanic methane as a cause of the carbon isotope excursion at the end of the Paleocene: Paleoceanography, 10, 965-971.

Dickens, G.R., Castillo, M.M., Walker, J.C.G., 1997, A blast of gas in the latest Paleocene: Simulating first-order effects of massive dissociation of oceanic methane hydrate: Geology, 25, 259-262.

Ellis, B.F., Messina, A.R., 1940, Catalogues of Micropalaeontology: Foraminifers, Ostracoda, Diatoms: New York, Paleontology Press.

Giusberti, L., Rio, D., Agnini, C., Backman, J., Fornaciari, E., Tateo, F., Oddone, M., 2007, Mode and tempo of the Paleocene-Eocene thermal maximum in an expanded section from the Venetian pre-Alps: Geological Society of America Bulletin, 119, 391-412.

Guernet, C., Molina, E., 1997, Les Ostracodes et le passage Paléocène-Eocène dans les Cordillères Bétiques (coupe de Caravaca, Espagne): Geobios, 30, 31-43.

Jorissen, F.J., De Stigter, H.C., Widmark, J.G.V., 1995, A conceptual model explaining benthic foraminiferal microhabitats: Marine Micropaleontology, 22, 3-15.

Jorissen, F.J., Fontanier, C., Thomas, E., 2007, Paleoceanographical proxies based on deep-se benthic foraminiferal assemblage characteristics, *in* Hillaire-Marcel, C., De Vernal, A. (eds.), Paleoceanography of the Late Cenozoic: Elsevier, Methods in Late Cenozoic, Paleoceanography, 1, 875 pp.

Kaiho, K., Takeda, K., Petrizzo, M.R., Zachos, J.C., 2006, Anomalous shifts in tropical Pacific planktonic and benthic foraminiferal test size during the Paleocene-Eocene thermal maximum: Palaeogeography, Palaeoclimatology, Palaeoecology, 237, 456-464.

Kaminski, M.A., Boersma, A, Tyszka, J., Holbourn, A.E.L., 1995, Response of deep-water agglutinated foraminifers to dysoxic conditions in the California borderland basins, *in* Kaminski, M.A., Geroch, S., Gasinski, M.A. (eds.), Proceedings of the Fourth International Workshop on Agglutinated Foraminifers: Grzybowski Foundation Special Publication 3, 131-140.

Kaminski, M.A., Gradstein, F.M., 2005, Atlas of Paleogene Cosmopolitan deep-water Agglutinated Foraminifers: Grzybowski Foundation Special Publication 10, 1-547.

Katz, M.E., Miller, K.G., 1991, Early Paleogene benthic foraminiferal assemblage and stable isotope composition in the Southern Ocean, *in* Ciesielski, P.F., Kristoffersen, Y., Clement, B., Blangy, J.P., Bourrouilh, R., Crux, J.A., Fenner, J.M., Froelich, P.N., Hailwood, E., Hodell, D., Katz, M.E., Ling, H.Y., Mienert, J., Muller, D., Mwenifumbo, C.J., Nobes, D.C., Nocchi, M., Warnke, D.A., Westall F. (eds.), Subantarctic South Atlantic: Proceedings of the Ocean Drilling Program, Scientific Results, 114, 481-512.

Kelly, D.C., Bralower, T.J., Zachos, J.C., 1998, Evolutionary consequences of the latest Paleocene thermal maximum for tropical planktonic foraminifers: Palaeogeography, Palaeoclimatology, Palaeoecology, 141, 139-161.

Kelly, D.C., Bralower, T.J., Zachos, J.C., Premoli Silva, I., Thomas, E., 1995, Rapid diversification of planktonic foraminifers in the tropical Pacific (ODP Site 865) during the late Paleocene thermal maximum: Geology, 24, 423-426.

Kennett, J.P., Stott, L.D., 1991, Abrupt deep-sea warming, palaeoceanographic changes and benthic extinctions at the end of the Palaeocene: Nature, 353, 225-229.

Kuhnt, W., Kaminski, M.A., 1997, Cenomanian to Lower Eocene deep-water agglutinated foraminifers from the Zumaya section, northern Spain: Annales Societatis Geologorum Poloniae, 67, 257-270.

Lu, G., Keller, G., Adatte, T., Ortiz, N., Molina, E., 1996, Long-term (10^5) or short-term (10^3) $\delta^{13}C$ excursion near the Palaeocene-Eocene transition: evidence from the Tethys: Terra Nova, 8, 347-355.

Molina, E., Canudo, J.I., Martínez-Ruiz, F., Ortiz, N., 1994, Integrated stratigraphy across the Paleocene-Eocene boundary at Caravaca, southern Spain: Eclogae Geologicae Helvetiae, 87, 47-61.

Molina, E., Arenillas, I., Pardo, E., 1999, High resolution planktic foraminiferal biostratigraphy and correlation across the Paleocene/Eocene boundary in the Tethys: Bulletin de la Société géologique de France, 174, 521-530.

Molina, E., Angori, E., Arenillas, I., Brinkhuis, H., Crouch, E.M., Luterbacher, H., Monechi, S., Schmitz, B., 2003, Correlation between the Paleocene/Eocene boundary and the Ilerdian at Campo, Spain: Revue de Micropaléontologie, 46, 95-109.

Moore, E.A., Kurtz, A.C., 2008, Black carbon in Paleocene-Eocene boundary sediments: A test of biomass combustion as the PETM trigger: Palaeogeography, Palaeoclimatology, Palaeoecology, 267, 147-152.

Nomura, R., 1991, Paleoceanography of Upper Maastrichtian to Eocene benthic foraminiferal assemblages at sites 752, 753, and 754, Eastern Indian Ocean, *in* Peirce, J., Weissel, J., Taylor, E., Alt, J., Dehn, J., Driscoll, N., Farrell, J., Fourtanier, E., Frey, F., Gamson, P.D., Gee, J.S., Gibson, I.L., Janecek, T., Klootwijk, C., Lawrence, J.R., Littke, R., Newman, J.S., Nomura, R., Owen, R.M., Pospichal, J.J., Rea, D.K., Resiwati, P., Saunders, A.D., Smit, J., Smith, G.M., Tamaki, K., Weis, D., Wllkinson, G. (eds.), Broken Ridge and Ninetyeast Ridge: Proceedings of the Ocean Drilling Program, Scientific Results, 121, 3-29.

Ortiz, N., 1995, Differential patterns of benthic foraminiferal extinctions near the Paleocene/Eocene boundary in the North Atlantic and the western Tethys: Marine Micropaleontology, 26, 341-359.

Ortiz, S., 2006, Análisis de eventos del Paleógeno con foraminíferos bentónicos. Taxonomía, reconstrucción paleoambiental y aplicación cronoestratigráfica: Zaragoza, Spain, Universidad de Zaragoza, Ph.D. Thesis, (unpublished), 380 pp.

Orue-Etxebarria, X., Apellaniz, E., Baceta, J.I., Coccioni, R., di Leo, R., Dinares-Turrell, J., Galeotti, S., Monechi, S., Núñez-Betelu, K., Pares, J.M., Payros, A., Pujalte, V., Samso, J.M., Serra-Kiel, J., Schmitz, B., Tosquella, J., 1996, Physical and biostratigraphic analyses of two prospective Paleocene-Eocene boundary stratotypes in the intermediate-deep water Basque Basin, western Pyrenees: the Trabakua Pass and Ermua sections: Neues Jahrbuch für Geologie und Paläontologie, Abhandlungen, 201, 179-242.

Pardo, A., Keller, G., Molina, E., Canudo, J.I., 1997, Planktic foraminiferal turnover across the Paleocene-Eocene transition at DSDP Site 401, Bay of Biscay, North Atlantic: Marine Micropaleontology, 29, 129-158.

Röhl, U., Bralower, T.J., Norris, R.D., Wefer, G., 2000, New chronology for the late Paleocene thermal maximum and its environmental implications: Geology, 28, 927-930.

Schmitz, B., Asaro, F., Molina, E., Monechi, S., Von Salis, K., Speijer, R.P., 1997, High-resolution iridium, $\delta^{13}C$, $\delta^{18}O$, foraminifers and nannofossil profiles across the latest Paleocene benthic extinction

event at Zumaya, Spain: Palaeogeography, Palaeoclimatology, Palaeoecology, 133, 49-68.

Schmitz, B., Pujalte, V., Nuñez Betelu, K., 2001, Climate and sea level perturbations during the initial Eocene thermal maximum: evidence from siliciclastic units in the Basque Basin (Ermua, Zumaia and Trabakua Pass), northern Spain: Palaeogeography, Palaeoclimatology, Palaeoecology, 165, 299-320.

Shackleton, N.J., Hall, M.A., Bleil, U., 1985, Carbon-isotope stratigraphy, Site 577, *in* Hearth, G.R., Burckle, L.H., D'Agostino, A.E., Horai, K., Janecek, T., Koizumi, I., Krissek, L.A., Lenôtre, N., Monechi, S., Morley , J.J., Wright, A.A. (eds.), Initial Reports of the Deep Sea Drilling Project 86, 503-511.

Schnitker, D., 1979, Cenozoic deep-water benthic foraminifers, Bay of Biscay, *in* Montadert, L., Roberts, D.G., Auffret, G.A., Bock, W.D., Dupeuble, P.A., Hailwood, E.A., Harrison, W.E., Kagami, H., Lumsden, D.N., Muller, C.M., Schnitker, D., Thompson, R.W., Thompson, T.L., Timofeev, P.P. (eds.), Initial Reports of the Deep Sea Drilling Project 48, 377-413.

Sluijs, A., Brinkhuis, H., Schouten, S., Bohaty, S.M., John, C.M., Zachos, J.C., Reichart, G.J., Sinninghe Damsté, J.S., Crouch, E., Dickens, G.R., 2007, Environmental precursors to rapid light carbon injection at the Palaeocene/Eocene boundary: Nature, 450, 1218-1221.

Speijer, R.P., 1994, Extinction and recovery patterns in benthic foraminiferal paleocommunities across the Cretaceous/Paleogene and Paleocene/Eocene Boundaries: Geologica Ultraiectina, 124, 1-191.

Speijer, R.P., Wagner, T., 2002, Sea-level changes and black shales associated with the late Paleocene thermal maximum: Organic-geochemical and micropaleontologic evidence from the southern Tethyan margin (Egypt-Israel), *in* Koeberl, C., MacLeod, K.G. (eds.), Catastrophic Events and Mass Extinctions: impacts and beyond: Boulder, Colorado: Geological Society of America, Special Paper 356, 533-549.

Speijer, R.P., Schmitz B., Van Der Zwaan, G.J., 1997, Benthic foraminiferal extinction and repopulation in response to latest Paleocene Tethyan anoxia: Geology, 25, 683-686.

Sztràkos, K., 1996, Le Thanetien supérieur et l'Yprésien du Bassin de l'Adour (Aquitaine, France). Stratigraphie et Paléoenvironnement. Étude des foraminifers: Cahiers de Micropaléontologie, 10, 25-63.

Takeda, K., Kaiho, K., 2007, Faunal turnovers in central Pacific benthic foraminifera during the Paleocene-Eocene thermal maximum: Palaeogeography, Palaeoclimatology, Palaeoecology, 251, 175-197.

Thomas, E., 1990, Late Cretaceous-early Eocene mass extinctions in the deep sea, *in* Sharpton, V.L., Ward, P.D. (eds.), Global Catastrophes in Earth History: An Interdisciplinary Conference on Impacts, Volcanism, and Mass Mortality: Geological Society of America, Special Paper 247, 481-495.

Thomas, E., 2003, Extinction and food at the sea floor: a high-resolution benthic foraminiferal record across the Initial Eocene Thermal Maximum, Southern Ocean Site 690, *in* Wing, S.L., Gingerich, P., Schmitz, B., Thomas, E. (eds.), Causes and Consequences of Globally Warm Climates in the Early Paleogene: Geological Society of America, Special Paper 369, 319-332.

Thomas, E., 2007, Cenozoic mass extinctions in the deep sea; what disturbs the largest habitat on Earth?, *in* Monechi, S., Coccioni, R., Rampino M. (eds.), Large Ecosystem Perturbations: Causes and Consequences: Geological Society of America, Special Paper 424, 1-23.

Thomas, E., Shackleton, N.J., 1996, The Paleocene-Eocene benthic foraminiferal extinction and stable isotopic anomalies: Geological Society London, Special Publication 101, 401-441.

Thomas, E., Zachos, J.C., Bralower, T.J., 2000, Deep-sea environments on a warm earth: latest Paleocene-early Eocene, *in* Huber, B.T., MacLeod, K.G., Wing, S.L. (eds.), Warm Climates in Earth History: Cambridge, Cambridge University Press, 132-160.

Tjalsma, R.C., 1977, Cenozoic Foraminifers from the South Atlantic, DSDP leg 36, *in* Barker, P., Dalziel, I.W.D., Dinkelman, M.G., Elliott, D.H., Gombos, J.A.M., Lonardi, A., Plafker, G., Tarney, J., Thompson, R.W., Tjalsma, R.C., Von Der Borch, C.C., Wise, J.S.W. (eds.), Initial Reports of the Deep Sea Drilling Project 36, 493-518.

Tjalsma, R.C., Lohmann, G.P., 1983, Paleocene-Eocene bathyal and abyssal benthic foraminifers from the Atlantic Ocean: Micropaleontology, Special Publication 4, 1-90.

Van Morkhoven, E.P.C.M., Berggren, W.A., Edwards, A.S., 1986, Cenozoic cosmopolitan deep-water benthic foraminifers: Bulletin des Centres de Recherche Exploration-Production Elf-Aquitaine, 11, 1- 421.

Westerhold, T., Röhl, U., Laskar, J., Bowles, J., Raffi, I., Lourens, L.J., Zachos, J.C., 2007, On the duration of magnetocrons C24r and C25n and the timing of early Eocene global warming events: implications from the ocean Drilling Program Leg 208 Walvis Ridge depth transect: Paleoceanography, 22, (PA2201), doi: 10.1029/2006PA001322.

Westerhold, T., Röhl, U., Raffi, I., Fornaciari, E., Monechi, S., Reale, V., Bowles, J. Evans, H.F., 2008, Astronomical calibration of the Paleocene time: Palaeogeography, Palaeoclimatology, Palaeoecology, 257, 377-403.

Zachos, J.C., Pagani, M., Sloan, L., Thomas, E., Billups, K., 2001, Trends, rythms, and aberrations in global climate 65 Ma to Present: Science, 292, 686-693.

Zachos, J.C., Röhl, U., Schellenberg, S.A., Sluijs, A., Hodell, D.A., Kelly, D.C., Thomas, E., Nicolo, M., Raffi, I., Lourens, L.J., McCarren, H., Kroon, D., 2005, Rapid acidification of the ocean during the Paleocene-Eocene Thermal Maximum: Science, 308, 1611-1615.

Zachos, J.C., Wara, M.W., Bohaty, S., Delaney, M.L., Petrizzo, M.R., Brill, A., Bralower, T., Premoli-Silva, I., 2003, A transient rise in tropical sea surface temperature during the Paleocene-Eocene Thermal Maximum: Science, 302, 1551-1554.

Zeebe, R.E., Zachos, J.C., 2007, Reversed deep-sea carbonate ion basin gradient during Paleocene-Eocene thermal maximum: Paleoceanography, 20, (PA3201), 1-17.